European Journal of Pharmaceutical Sciences 172 (2022) 106140

Contents lists available at ScienceDirect

European Journal of Pharmaceutical Sciences

journal homepage: www.elsevier.com/locate/ejps

System model driven selection of robust tablet manufacturing processes based on drug loading and formulation physical attributes

Leah R. White, Matthew Molloy *, Robert J. Shaw, Gavin K. Reynolds

Oral Product Development, Pharmaceutical Technology & Development, Operations, AstraZeneca, Macclesfield, UK

ARTICLE INFO

Keywords:
Formulation design
System model
Design space
Pharmaceutical process

ABSTRACT

Mechanistic process modeling presents an opportunity to reduce experimental burden, enabling relationships between process parameters and product attributes to be mapped out using *in-silico* experiments. A system model of a pharmaceutical tablet manufacturing process comparing dry granulation with direct compression is developed to answer key material and process design questions. The system model links API physical properties and formulation to process parameters to map out the robust operating space. To demonstrate the application of the model, several drug product formulation design questions were considered:

- Which processing route is the most robust given the API material properties and dosage requirements?
- How does drug loading and tablet size impact the robustness of the manufacturing process?
- What process settings are required for a robust manufacturing route for the API material properties and drug loading requirements?

A computational framework was developed using the system models to generate process classification and design space maps to aid robust pharmaceutical formulation and process decision making. Process classification maps were produced to assess the feasibility of roller compaction and direct compression for different material properties and formulations. Constraints on the critical quality attributes of the intermediate and final products were defined using the Manufacturing Classification System. Design space maps presented here demonstrate how system models can be used to support formulation and process design. The design space maps illustrate how the process operating space can be increased or decreased as the API mass fraction is varied.

The process design and selection system model demonstrate how an understanding of the API physical properties can be used to model the impact of formulation and process design. Furthermore, these models can be instrumental in the dialogue with colleagues developing the API in order to set the requirements of the API physical properties to ensure successful and robust formulation and process designs.

1. Introduction

Understanding the impact of formulation design and material properties on the pharmaceutical drug product manufacturing process is critical for ensuring product and process robustness. When developing an oral solid dosage (OSD) product, design decisions must be made to select a suitable process route and formulation, which are highly dependent on the physical properties of the active pharmaceutical ingredient (API). Making non-optimal decisions in the design phase can result in quality and cost issues during later stages of development and in commercial manufacture. The industry transformation in R&D pipeline success, rapid clinical programs and expedited regulatory approval is putting significant pressure on traditional pharmaceutical development and scale-up timelines. Ensuring rapid design decisions yield a robust formulation and process that is resilient to variability in API properties and processing conditions is now becoming a critical capability of pharmaceutical development.

* Corresponding author.
E-mail address: matthew.molloy@astrazeneca.com (M. Molloy).

https://doi.org/10.1016/j.ejps.2022.106140
Received 21 October 2021; Received in revised form 1 February 2022; Accepted 2 February 2022
Available online 8 February 2022

Nomenclature

P_{max}	peak roll pressure during roller compaction
R_f	roll force
W	roll width
D	roll diameter
α	nip angle
δ_E	effective angle of internal friction
Φ_W	wall friction angle
θ	angular roll position
S	roll separation
K_{RC}	material compressibility constant for roller compaction
γ_0	pre-consolidation relative density
ε_{tablet}	tablet porosity
K_T	compressibility constant
P_T	compaction pressure
P_0	theoretical pressure for zero porosity
x_{API}	mass fraction of API
m_{tablet}	tablet mass
$\rho_{blend,bulk}$	blend bulk density
$A_{cs,tablet}$	tablet cross-sectional area
T	tensile strength
T	tensile strength at zero porosity
k_b	bonding capacity
ε_{ribbon}	ribbon porosity
c	loss of compactability coefficient
T_{ribbon}	ribbon tensile strength
$y_{i,particle}$	particle volume fraction for component *i*
x_i	mass fraction of component *i*
$\rho_{i,particle}$	particle density of component *i*
$\rho_{blend,particle}$	blend particle density
φ_i	material property of component *i*
$\varphi_{blend,mass}$	mass weighted blend material property
$\varphi_{blend,PV}$	particle volume weighted blend material property
$\varphi_{blend,BV}$	bulk volume weighted blend material property
$y_{i,SA}$	surface area weighted volume fraction of component *i*
$D_{[3,2]i}$	sauter mean diameter of component *i*

The Manufacturing Classification System (MCS) was developed to rank the feasibility of oral solid dosage (OSD) processing routes based on chemical-physical and mechanical characteristics APIs and the formulation (Leane et al., 2015, 2018) with the aim of providing a systematic approach for making formulation and process selection decisions. The MCS defines four possible processing routes to produce OSD products: direct compression (DC) (class I), dry granulation (DG) (class II), wet granulation (WG) (class III) and other technologies (OT) (class IV), each with increasing processing steps, complexity and development and manufacturing costs (Iacocca et al., 2010; Leane et al., 2015). All processing routes have the potential to be run continuously. Continuous manufacturing (CM) is advantageous to the pharmaceutical industry due to reduced material handling steps, improved flexibility and the ability to integrate quality by design (QbD) principles (Mascia et al., 2013; Vercruysse and Delaet, 2013; Lee et al., 2015, 2016). CM also provides an opportunity to implement process analytical technologies (PAT) which enables inline process and product monitoring for enhanced product quality assurance (Palmer et al., 2020). For a set of API properties, the MCS framework enables feasible manufacturing routes to be assessed and the formulation designed accordingly to maximize the uptake of CM (Leane et al., 2018).

The introduction of quality by design (QbD) has led to enhanced material and process understanding by utilizing Design of Experiments (DoE) to explore the design space and establish the relationships between process parameters and product attributes (Lee et al., 2020). DoE has also been combined with multivariate modeling to experimentally map out the design space of tablet manufacturing processes for different formulations and used to make design decisions about the formulation and manufacturing route (Souihi et al., 2013; Pishnamazi et al., 2019; Yu et al., 2019; Palmer et al., 2020). The DoE approach requires extensive experimental work which is resource and cost-intensive (Pohl and Kleinebudde, 2020) and also limits the rate at which understanding can be generated early in development when there is often limited API available.

Mechanistic process modeling presents an opportunity to reduce experimental burden, enabling relationships between process parameters and product attributes to be mapped out using *in-silico* experiments. Individual material and process models cannot capture the interdependency between unit operations or the impact of material properties on processing behavior. Connecting individual unit operation and material models together to form a system model enables the relationships between unit operations and materials to be explored in a single model. Gavi and Reynolds (2014) developed a system model for a dry granulation (DG) tablet manufacturing process, demonstrating how a relatively small dataset could be used to explore the feasible operating space of the system. However, the unit operation models require material parameter calibration and therefore it is difficult to explore the impact of changes to the formulation design without generating additional process data to carry out further parameter calibration. Existing system models are also limited to a single manufacturing route and do not explore the impact of material properties and formulation on the feasibility of different manufacturing routes. To our best knowledge, no models yet exist which combine material models and unit operations into a full system model to explore the impact of API and excipient properties on drug product manufacturing robustness.

In this paper, a system model of a pharmaceutical tablet manufacturing process comparing dry granulation with direct compression is developed to answer key material and process design questions. The key product quality attributes are ribbon tensile strength, tablet porosity and tablet tensile strength. The roller compactor model is taken from literature (Johanson, 1965; Reynolds et al., 2010). The models for the tablet porosity and tensile strength are a combination and extension of previous literature which consider both the loss in compressibility of the material associated with dry granulation (Gavi and Reynolds, 2014) and the compressibility behavior of a powder mixture based on its components (Reynolds et al., 2017). As the impact of component material properties and formulation were a key question to ask of the system model, mixture models were validated to predict the blend particle density, blend bulk density and blend flow function coefficient (FFC) from the formulation components.

The objective of this work was to develop a system model to aid formulation and processing design decisions that meet the requirements of the quality target product profile (QTPP). The motivation for the model was to specifically inform the selection between continuous direct compression (CDC) and roller compaction (RC) manufacturing routes. However to simplify construction of the system model, the primary criteria for selection of the CDC process was related to performance in the tablet press and therefore this process route is referred to as direct compression (DC). Analysis of the model aims to allow the formulator to understand the risk associated with a given processing route in achieving the critical quality attributes (CQA) of the product through in-silico exploration of the potential critical material attributes (CMA) and critical process parameters (CPP) and make appropriate formulation choices to maximize process robustness. Additionally, the aim of the system model was to link API physical properties and formulation to process parameters to map out the robust operating space. To

demonstrate the application of the model, several drug product formulation design questions were considered:

- Which processing route is the most robust given the API material properties and dosage requirements?
- How does drug loading and tablet size impact the robustness of the manufacturing process?
- What process settings are required for a robust manufacturing route for the API material properties and drug loading requirements?

The paper has the following structure. First, an overview of the mixture models for powder bulk are described. These models allow changes in the formulation composition to influence the overall system model so that formulation and process changes can be simulated. An overview is then given of the process models used to describe the unit operations. The experimental work used to build and calibrate the models is described and the methodology used to calibrate both the material and process models is outlined. Finally, system analysis is performed on the model to define the impact of processing parameters, material properties and formulation decisions on the suitability of processing routes and the robustness of the intermediate and final products. Process classification maps and design space maps are produced to visualize the output of the analysis and aid product formulation and manufacturing design decisions.

2. Theory

The tablet manufacturing system model is composed of both process models and material models. The process models describe the interaction between the materials and the physical equipment through which it is being processed. The material models consider physical attributes and behavior of raw materials, intermediates and product as a function of the individual components material properties of the formulation.

2.1. Process models

2.1.1. Roller compactor

In the Roller Compactor, the powder blend is fed through two counter-rotating rollers and compacted to form a ribbon. Reynolds et al. (2010) describe a model, based on that of Johanson (1965), which was utilized in the system model to describe the behavior of the roller compactor. The model is straightforward to implement as it requires only a few measurements of the powder bulk properties (angle of wall friction and effective angle of internal friction) and two lumped parameters describing the compaction properties, that need to be fitted from experimental roller compaction data. The model provides a relationship between process parameters, equipment geometry and powder material properties to determine the ribbon relative density, γ_R, using the following equation.

$$\gamma_R = \gamma_0 \, P_{max}^{1/K_{RC}} \tag{1}$$

where γ_0 is the pre-consolidation relative density of the ribbon, K_{RC} is the compressibility constant for partially confined compression and P_{max} is peak roll pressure at minimum separation applied during RC defined by

$$P_{max} = \frac{2R_f}{WD\int_{\theta=0}^{\theta=\alpha(\delta_E,\phi_W,K_{RC})} [(S/D)/((1+(S/D)-\cos\theta)\cos\theta)]^{K_{RC}}\cos\theta \, d\theta} \tag{2}$$

where R_f is the force applied to the rolls, W is the roll width, D is the roll diameter, S is the roll separation or gap, θ is the angular roll position, α is the nip angle, δ_E is the effective angle of internal friction and ϕ_W is the angle of wall friction. The model is calibrated with experimental data by fitting two parameters: γ_0 and K_{RC}. The parameters are fitted with experimental ribbon relative density data as a function of applied roll pressure. In order to simulate the influence of formulation changes on the RC process, the two RC model parameters were fitted as a function of API mass fraction.

2.1.2. Tablet press

For a dry granulation manufacturing process, the granules are compacted into tablets in the tablet press. In a direct compression manufacturing process, the loose powder blend is directly compacted into tablets.

A modified version of the Gurnham equation is used to represent the compressibility of a powder in a tablet press

$$\varepsilon_{tablet} = -\frac{1}{K_T} ln\left(\frac{P_T}{P_0}\right) \tag{3}$$

where ε_{tablet} is the tablet porosity, K_T is the compressibility constant for confined compression, P_T is the applied pressure and P_0 is the theoretical pressure required to produce a zero porosity compact. The compressibility parameters, K_T and P_0, are determined for each component in the formulation using experimental tablet porosity as a function of tablet compaction pressure data. In order to account for changes in formulation, specifically API mass fraction, the Reynolds et al. (2017) compressibility model was applied to Eq. (3) to take account of the relative contribution of the constitutive components.

Tablet dosage: API mass fraction and dosage of the tablet were important factors in the system model, particularly when developing process selection tools. The dosage of a tablet was calculated by Eq. (4)

$$tablet\ dosage = x_{API} m_{tablet} \tag{4}$$

where x_{API} is the mass fraction of the API and m_{tablet} is the mass of the tablet.

Die fill level: The tablet size, shape and API mass fraction affect whether a formulation is suitable for direct compression in the tablet press. During direct compression, the tablet die is filled with the powder blend. The level in the die which the tablet reaches depends on the bulk density of the blend, the cross-sectional area of the tablet, $A_{cs,tablet}$ and the mass of the powder required to make the tablet. The level which is reached by the powder blend in the tablet die is critical to product robustness in the tablet press and is estimated by the following equation, which assumes the relative volume of the lower cup is negligible.

$$die\ fill\ level = \frac{m_{tablet}}{\rho_{blend,bulk}\ A_{cs,tablet}} \tag{5}$$

For DC, a low bulk density of the powder blend can significantly impact the feasibility of processing if the required mass is unable to be accommodated by the die. API particle engineering (Chattoraj and Sun, 2018) and changes to formulation through adjusting the API mass fraction and excipients are the primary strategies for overcoming poor process robustness associated with poor API bulk properties. Where the die fill level poses a significant risk to the direct compression process robustness, the densification of the powder through a dry granulation process can be used to increase the bulk density and reduce the risk of the material not fitting in the die.

2.2. Material models

2.2.1. Tablet tensile strength

The compactability of a powder is defined as the change in tensile strength of a powder as a function of powder density (Reynolds et al., 2017). The Reynolds et al. (2017) model uses the Ryshkewitch-Duckworth equation to model the compactability of a directly compressed powder

$$T = \overline{T} e^{-k_b \varepsilon_{tablet}} \tag{6}$$

where T is the tensile strength, $\overline{T}$ (MPa) is the tensile strength at zero

porosity and k_b is the bonding capacity of the blend. This model was used for the tablet press in the direct compression system model.

Building on the 'loss of compactability' work by Farber et al. (2008), Gavi and Reynolds (2014) modified the Ryshkewith-Duckworth compactability model (Duckworth, 1953) to account for the loss in compactability of the material during roller compaction. Although the Gavi and Reynolds (2014) model corrects for the loss of compactability, different materials tend to exhibit different extents of loss in compactability due differences in particle size, morphology, shape, surface roughness, fragmentation and deformation (Sun and Kleinebudde, 2016). Therefore, a correction parameter, *c*, was added to account for differences in extent of loss in compactability and improve the model to give

$$T = \overline{T}e^{-k_b\varepsilon_{tablet}} - c\overline{T}e^{-k_b\varepsilon_{ribbon}} \tag{7}$$

where T is the tensile strength of the tablet, $\overline{T}$ is the tensile strength at zero porosity, k_b is the bonding capacity of the blend, ε_{ribbon} is the ribbon porosity and c is the loss in compactability coefficient. This coefficient is a phenomenological factor used to capture the extent of loss of compactability exhibited due to differences in the material properties that can be fitted to different formulations.

The compactability parameters, $\overline{T}$ and k_b, were fitted for each component in the formulation using experimental data and the Reynolds et al. (2017) model was applied to Eqs. (6) and (7) to calculate the DC and RC tablet properties for different API mass fractions.

The purpose of a roller compaction process is to produce granules, which are created by milling a well-formed ribbon. Calculating the tensile strength of the ribbon can be used as in indicator of the generation of a coherent, robust ribbon. The ribbon tensile strength, T_{ribbon}, can be calculated using the relationship in Eq. (6), but using the ribbon porosity, (Eq. (8)):

$$T_{ribbon} = \overline{T}e^{-k_b\varepsilon_{ribbon}} \tag{8}$$

2.2.2. Blend particle density

The particle density, also known as true density, of a material is the density of the material, excluding the voids between particles. A volume-weighted average was used to determine the particle density of the blend based on the particle density of the components. The particle volume fraction of each component, $y_{i,particle}$, is shown in Eq. (9)

$$y_{i,particle} = \frac{x_i}{\rho_{i,particle}} \tag{9}$$

where x_i is the mass fraction of component i in the formulation and $\rho_{i,particle}$ is the particle density of component i. The blend particle density, $\rho_{blend,particle}$, was then calculated by Eq. (10)

$$\rho_{blend,particle} = \frac{1}{\sum y_{i,particle}} \tag{10}$$

2.2.3. Bulk property mixture models

Two material properties of the blend were calculated from the formulation components: bulk density and the flow function coefficient (FFC). The bulk density of the blend is defined as the mass per unit volume of the powder mixture including the intra- and inter-particle voids. It is a key property for process robustness during tablet manufacturing. The prediction of a bulk density mixture from its components is not straightforward as it is influenced by particle shape, packing and constituent particle density.

The flow of a powder is critical to process robustness. The FFC, typically measured using a shear cell, is commonly used to describe powder flowability. Poor flowability presents a processing risk in a direct compression process due to segregation occurring during transport to the tablet press and inconsistent tablet press die filling resulting in tablet weight variability. Poor flowability of a blend in an RC process can lead to bridging, ratholing and segregation at the entrance to the roller compactor, which can severely impact process robustness.

As a pragmatic approach, we evaluated several simple mixture rules for the materials used in this paper and the models with the best performance were selected. Here ϕ is the material property being predicted: bulk density or FFC.

Mass-weighted: The mass-weighted mixture model for calculating the blend material property is given by equation 11

$$\varphi_{blend,mass} = \sum x_i\ \varphi_i \tag{11}$$

where $\varphi_{blend,mass}$ is the mass-weighted component property of the mixture and φ_i is the material property of component i.

Particle volume-weighted: The particle-volume weighted mixture model for calculating the blend material property is given in Eq. (12)

$$\varphi_{blend,PV} = \sum\left(\frac{y_{i,particle}}{\sum y_{i,particle}} \times \varphi_i\right) \tag{12}$$

where $\varphi_{blend,PV}$ is the particle volume-weighted component property of the mixture.

Bulk volume-weighted: The bulk volume-weighted mixture rule can also be used to calculate the blend material properties. The bulk volume fraction of component i, $y_{i,bulk}$, was calculated by Eq. (13)

$$y_{i,bulk} = \frac{x_i}{\rho_{i,bulk}} \tag{13}$$

and the blend material property was calculated by Eq. (14)

$$\varphi_{blend,BV} = \sum\left(\frac{y_{i,bulk}}{\sum y_{i,bulk}} \times \varphi_i\right) \tag{14}$$

where $\varphi_{blend,BV}$ is the bulk volume-weighted component property of the mixture

Surface area volume-weighted: A surface area-weighted mixture rule was also evaluated to calculate the blend material properties. The Sauter mean diameter of each component, $D[3,2]_i$, was used to weight the particle volume of each component. The surface area-weighted volume fraction was then calculated by equation 15

$$y_{i,SA} = \frac{y_{i,particle}}{D[3,2]_i} \tag{15}$$

The surface area-weighted volume fraction for each component was used to determine the FFC of the blend

$$\varphi_{blend,SA} = \sum\left(\frac{y_{i,SA}}{\sum y_{i,SA}} \times \varphi_i\right) \tag{16}$$

2.3. System model description

The process models and material models were combined to form a system model which was constructed in gPROMS FormulatedProducts 2.0 (Siemens Process System Enterprise Ltd., UK). The flows of equipment parameters and material properties in and out of each model are shown in Fig. 1. The material properties of the API and excipient pass into the bulk property models which determine the material properties of the blend. The material properties pass into two pathways, RC and DC, which contain the relevant process models for the process.

For the roller compaction system model, the unit operations included are the roller compactor and the tablet press. In practice, blending and milling operations will also be incorporated into an RC process train. In order to simplify the system model, these unit operations were excluded due to the limited impact on the tablet properties. In the RC model, the blend density, porosity and friction coefficients as well as the mass fraction are used to determine the RC fitted parameters as a function of API mass fraction. In reality for the tablet compaction operation, milled

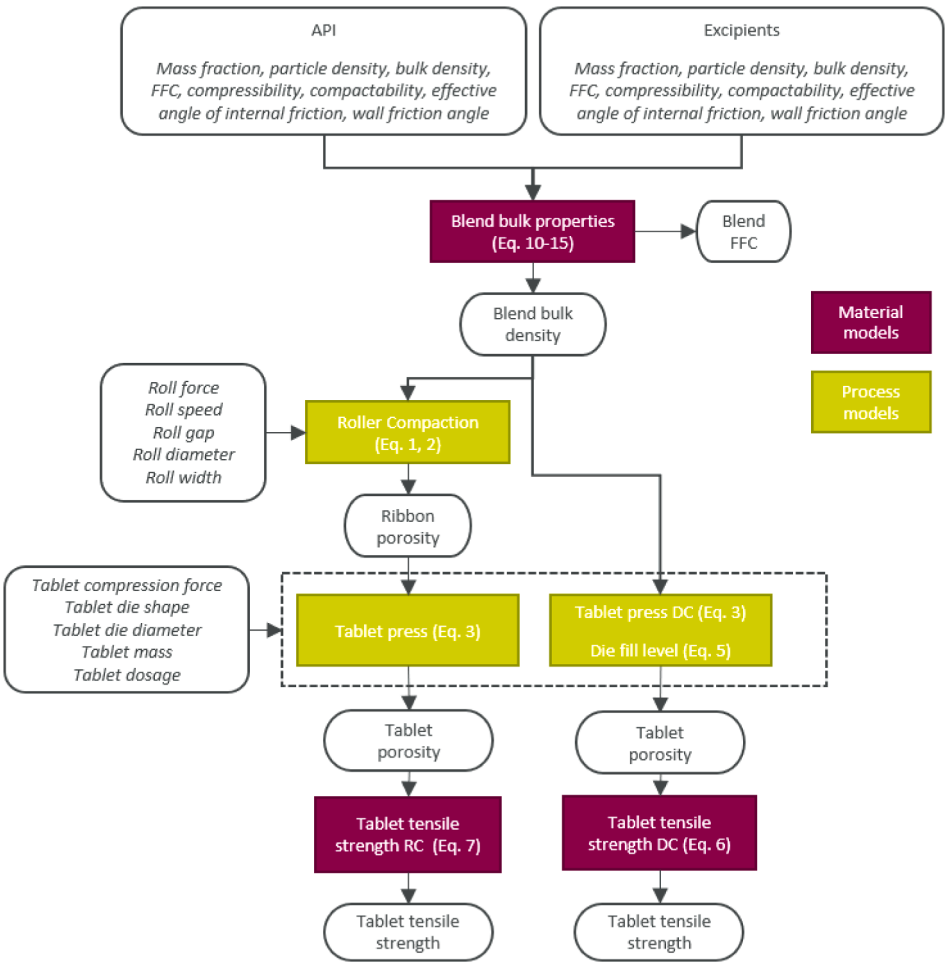

Fig. 1. Schematic of the system model.

granules flow into the tablet press but here we utilize the ribbon properties as an input to the tablet press model. It is assumed that the ribbon porosity is identical to the granule porosity as the granule size distribution including fines has very little influence on the compactability for a roller compaction process (Perez-Gandarillas et al., 2016). Furthermore, although blending with lubricant prior to the compaction process can have an impact on tensile strength, this is not modeled explicitly based on model validation using lubricated blends and an assumption that the blending process is sufficiently long to minimize variability (Kushner and Moore, 2010). The ribbon material properties flow into the tablet press model, alongside the mass fraction and compaction behavior of the components. The tablet porosity and tablet tensile strength are the main outputs of the tablet press model.

For the direct compression system model, only the tablet press unit operation is modeled. In practize feeding, blending and milling operations may also exist however these will have minimal impact on the tablet properties being considered for the purpose of this study. Specifically, feeding, blending and milling will primarily influence API content uniformity, which is not considered here. Lubrication is simplified using the same approach as roller compaction. In the DC pathway, the relevant component and blend properties pass directly into the tablet press model, which also includes the die fill level calculation. The calibration procedure for each unit operation is detailed in Section 4.

3. Experimental

Historical development data for a proprietary drug product was used to calibrate and validate the models. The dataset consisted of 90 API batches, with different physical properties, from which 124 bulk powder blends were created. 34 of these blends were included in 61 unique roller compacted runs. Of the 61 granule batches produced in the roller compactor, 37 granule batches were compacted in the tablet press at different compaction forces to generate compaction profiles and 6 granule batches were compacted at a single set point (Table 1). Data was also collated for the excipients in the formulation. All blends used for RC had the same formulation: 40% w/w API mass fraction with 2 fillers in a 50:50 ratio, a disintegrant and a lubricant. The remaining blends that were not roller compacted also had the same formulation except for two blends at 30% w/w API mass fraction and one blend at 15% w/w API mass fraction.

The particle size distribution of the API and excipient was measured using laser diffraction (Helos, Sympatec GmbH, Germany or Mastersizer 3000, Malvern Panalytical, United Kingdom). The particle density of the API and excipients was measured using a helium pycnometer (Accupyc 1330, Micromeritics, USA). The effective angle of internal friction, wall friction angle and flow function coefficient were measured using a ring

Table 1
Summary of experimental data used to calibrate the models.

Process Stage	API	Blend	Roller Compaction	Tablet Press
Number of Batches	90 batches	124 bulk powder blends	61 granule batches	Compaction profile: 37 granule batches Set point: 6 granule batches

shear tester at 4 kPa (RST-XS, Diet- mar Schultze, Germany). The bulk density of the API, excipients and blend was measured using a 50 ml measuring cylinder and recording the mass and volume of the powder.

Blends were roller compacted using one of two roller compactors depending on scale and location of manufacture: Mini-Pactor 250–25 (Gerteis Maschinen + Processengineering AG, Switzerland) or Pharmapaktor C 250 (Hosokawa Alpine AG, Germany). The Mini-Pactor was equipped with 25 mm wide, 250 mm diameter rolls with either smooth or power grip surface depending on the batch. The Pharmapaktor was equipped with 50 mm wide, 250 mm diameter rolls. The roll pressure varied between 4 and 8 kN/cm, the roll gap varied between 1.1 and 3 mm and the roll speed varied between 2 and 6 rpm. Granules were produced by a mill integrated into the roller compactor and the mill screen size was either 1 mm or 1.25 mm, depending on the batch.

Ribbon porosity was measured using the Geopyc 1360 (Micromeritics, USA). The Sotax HT100 tablet tester (Sotax, Switzerland) was used to measure the tablet weight, thickness and breaking force, which was used to calculate the tablet density and porosity using the true density. The tensile strength was estimated using the Pitt et al. (1989) equation.

Tablets were produced by compacting granules using one of two tablet presses depending on scale and location of manufacture: STY-L'One Evolution and a Fette 1200 tablet press (Fette Compacting). For each roller-compacted blend, the tablets were produced either at a target compaction force or at 5 compaction forces; the tablet press forces ranged between 5 and 23 kN. Two die shapes were used; the oval tablet tooling was concave with a length of 14.5 mm and a width of 7.25 mm, and the round shape tooling was concave with a 9 mm diameter. Compaction profiles were produced for each excipient using an ESH Compaction Simulator (Phoenix, Rubery Owen, Telford, England) and the resultant tablets were characterised. Tablet porosity was calculated from thickness and weight measurement.

4. Model calibration

4.1. Material model calibration

4.1.1. Blend bulk density

Experimental data for 124 blends from 90 API batches were used to calibrate the bulk density model. All blends had 40% w/w API mass fraction except for two blends at 30% w/w and one blend at 15% w/w API mass fraction. Due to the small weight percentage of the disintegrant and lubricant in the formulation, the disintegrant and lubricant were excluded from the evaluation. Mass-weighted (Eq. (11)), particle volume-weighted (Eq. (12)) and bulk volume-weighted (Eq. (14)) mixture rules were evaluated where ϕ was the bulk density of the material.

In Fig. 2, the validity of the models was assessed by comparing the experimental and predicted values and the RMSE of the mass-weighted, particle volume-weighted and bulk volume-weighted models was 59.5 kg m^{-3}, 58.2 kg m^{-3} and 50.7 kg m^{-3}, respectively.

Due to the particle density similarity of the API and the excipients, the particle volume-weighted mixture rule was almost identical to the mass-weighted mixture rule. Both models significantly overpredict the blend bulk density for low experimental bulk density values. At low API bulk densities, the contribution of the API increasingly dominates the blend bulk density, which is not capture by the model.

The bulk volume-weighted mixture rule significantly improved the fit of the model across the breadth of experimental blend bulk density and more accurately predicted lower bulk densities. The model was an improvement over the mass-weighted and particle volume-weighted models as at lower values of API bulk density, the API bulk density

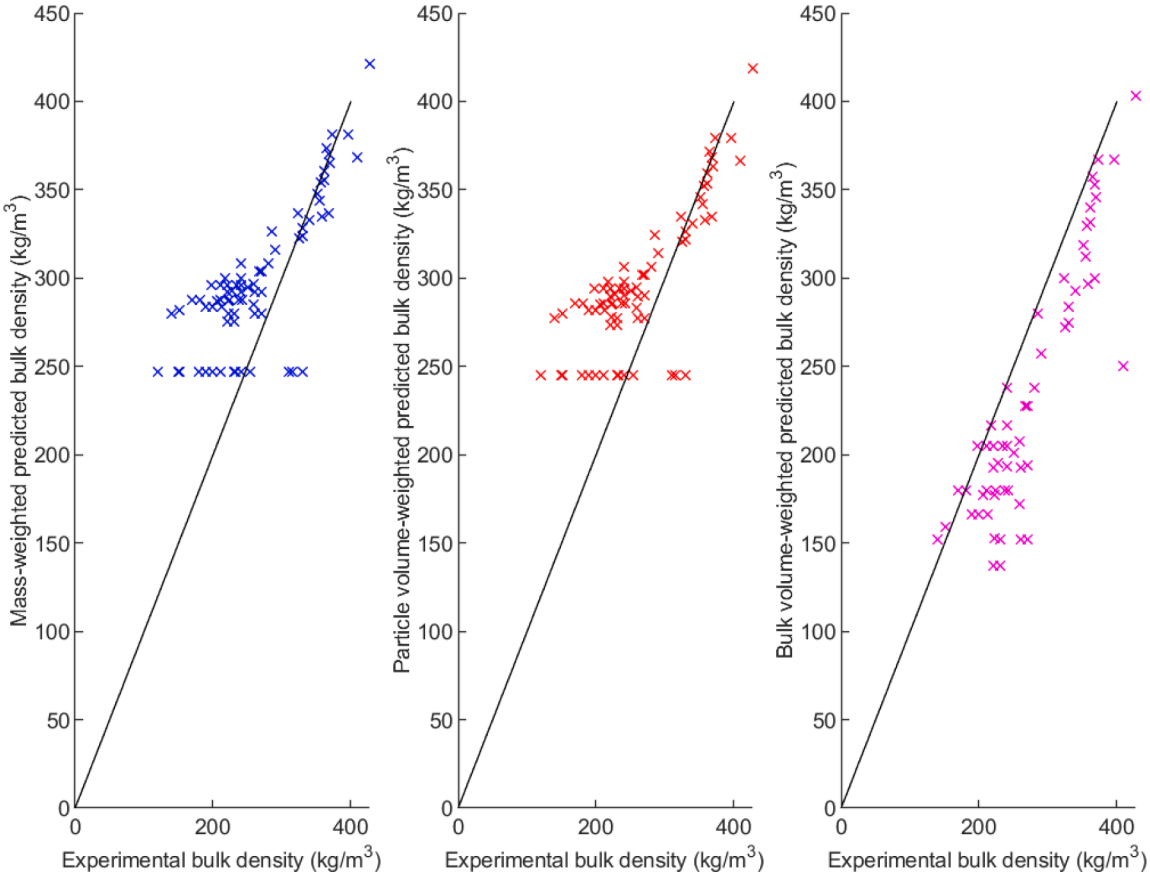

Fig. 2. Parity plots for blend bulk density mixture rules for the mass weighted, particle volume weighted and bulk volume weighted models.

dominates the mixture due to its higher volume at a constant API mass fraction. The bulk volume-weighted model may also account for the influence of particle shape as the data captures information on inter-particle voids which the mass-weighted and particle-volume weighted models fail to capture.

The bulk volume-weighted model exhibits bias by underpredicting the bulk density in the majority of cases, however this would be a conservative approach when used to de-risk selection of manufacturing processes. In contrast to the mass-weighted bulk density model, the low values of API bulk density dominate the bulk volume-weighted model due to the high API mass fraction and low bulk density. However, the bulk volume-weighted model still gives the best fit based on the RMSE of all the mixture models and is also most representative of the experimental bulk density across the full range of bulk densities, compared to the mass-weighted and particle volume-weighted models.

4.1.2. Blend flow function coefficient

Experimental data for 41 blends from 18 API batches were used to evaluate the blend FFC models. Mass-weighted (Eq. (11)), particle volume-weighted (Eq. (12)), bulk volume-weighted (Eq. (14)) and surface area-weighted (Eq. (16)) mixture rules were evaluated where ϕ was the FFC of the material.

The highest FFC value for the components in the formulation was 47.83. There is a risk with mixture rules that a very high value component could artificially dominate the mixture. The Schulze cohesion classification (Schulze, 2008) classifies FFC values greater than 10 as free-flowing and the magnitude to which a value exceeds 10 is not correlated to improved flowability. Therefore, the mixture rules were implemented twice and compared, where one of the components had an FFC of 10 or 47.83. Taking log to base 10 of all of the component FFC values was also implemented for all mixture rules to linearise the model and potentially improve the fit.

Predicting the exact FFC value is not critical but the prediction should be able to rank the materials in the correct order and fit the correct cohesion classification of the blend (Schulze, 2008). Comparison of the classification prediction was used as an additional assessment of the model validity, based on Table 2. The mass-weighted and particle-volume weighted models had very poor RMSE and% correct classification values (< 20%) so were not reported.

The lowest RMSE of 0.57 and the highest% correct classification of 73% for model 2 in Table 3 indicates that despite the noisy data associated with the experimental error, the SA-weighted mixture model with the high FFC excipient limited to 10 provided the best model fit.

4.2. Process model calibration

As detailed in Section 2, the process models require parameters to be calibrated. Models were required to represent the behavior of the processes at different API mass fraction values in the formulation. The calibration of the tablet press was carried out first as the mixture rules used in the Reynolds et al. (2017) model informed the calibration of the RC model as a function of API mass fraction.

4.2.1. Tablet press

The tablet press process model (Eq. (3)) predicts the porosity of the resultant tablet from the applied compaction pressure. The tablet tensile strength material model (Eq. (7)) predicts the tensile strength of the tablet based on the tablet porosity and ribbon porosity. Due to the close relationship between these models, the associated parameters, $\overline{T}$, k_b, P_0, K and c were calibrated together using the following methodology.

Theses parameters would be expected to change as the formulation composition changes due to differences in material compressibility and compactability. If sufficient data was available across many different API mass fractions, then these parameters could be determined in each case to develop a functional relationship. However, the historical dataset had extensive data only at an API mass fraction of 40% w/w and therefore the Reynolds et al. (2017) mixture model was used to extrapolate. To simplify the analysis, the system was considered as a binary mixture comprising the API and the bulk excipients. Compressibility and compactability parameters for the major individual excipient components were fitted from the compaction simulator data of the using Eqs. (3) and (6). The Reynolds et al. (2017) mixture model for tablet porosity and tensile strength was then used to fit surrogate grouped excipient compressibility and compactability parameters (Table 4). A single data point was available for a placebo formulation using a DC manufacturing process, equivalent to the grouped excipient mixture without the API. The difference between the experimental value and model prediction using the excipient parameters in Table 4 with a relative error of 2.3% for both the tablet porosity and tablet tensile strength prediction, which demonstrated a reasonable accuracy prediction of the 0% w/w API mass fraction formulation and provided confidence in the approach.

The API compressibility and compactability parameters were estimated by using the mixture model with 40% w/w API combined with the established excipient parameters and minimizing the sum of square errors (SSE) between the predicted and experimental values of tablet porosity and tablet tensile strength using a generalized reduced gradient (GRG) nonlinear method.

All of the available data was used to fit the compressibility and

Table 2
Cohesion classification for FFC values (Schulze, 2008).

FFC Value	Cohesion classification
10 < FFC	Free-flowing
4 < FFC < 10	Easy-flowing
2 < FFC < 4	Cohesive
1 < FFC < 2	Very cohesive
FFC < 1	Non-flowing

Table 3
The RMSE and percentage of predicted FFC values with the correct classification compared to the experimental classification for 8 different FFC mixture models.

Model Number	Mixture Rule	$\log_{10}$(FFC)	Limit FFC to 10	RMSE (-)	% correct classification
1	SA-weighted	No	No	1.26	65%
2	SA-weighted	No	Yes	0.57	73%
3	SA-weighted	Yes	No	0.65	57%
4	SA-weighted	Yes	Yes	0.73	50%
5	Bulk volume-weighted	No	No	6.78	14%
6	Bulk volume-weighted	No	Yes	1.78	65%
7	Bulk volume-weighted	Yes	No	0.99	65%
8	Bulk volume-weighted	Yes	Yes	2.52	67%

Table 4
Fitted compressibility and compactability values for both the API and the grouped excipients in the modified Reynolds et al. (2017) tablet press model.

Component	True density (calculated)(g/cc)	$\overline{T}$ (MPa)	k_b (-)	P_0 (MPa)	K (-)	c (-)
API	1.44	3.86	3.18	1600	26.7	0.61
Excipients	1.51	14.8	8.92	481	7.35	0.61

compactability models (Fig. 3). The RMSE was 0.51% w/w and 0.22 MPa for the compressibility and compactability models, respectively. To partly validate the model and assess the predictability, the dataset was split into a calibration set ($n = 72$) and a calibration set ($n = 15$). The RMSEC and RMSEP for the compressibility model compared with tablet porosity was 0.52% w/w and 0.53% w/w, respectively. The RMSEC and RMSEP for the compactability model compared with tablet tensile strength was 0.24 MPa and 0.21 MPa, respectively, both for the 40% w/w API mass fraction data. These metrics demonstrate the reliability of the model and the potential to utilize a smaller dataset for model calibration. The parameters fitted from the full dataset are used for the remainder of this study. Fig. 4 shows how the model predicts tablet porosity and tablet tensile strength as a function of API mass fraction. At higher API mass fractions, the tablets show a modest decrease in tensile strength, indicating that the compaction properties of the API are not significantly worse than the excipients in this case.

4.2.2. Roller compaction

The roller compaction process model requires two parameters, γ_0 and K_{RC}, to be calibrated. These parameters are related to the bulk material behavior in the roller compactor and are expected to vary as the drug load in the formulation is varied. Other parameters in the roller compactor model are the flow properties; δ_E and ϕ_W. Reynolds et al. (2010) demonstrated that the roller compactor model only showed a small sensitivity to these parameters. Therefore, δ_E and ϕ_W were kept constant (Table 5) regardless of API mass fraction as any changes to the parameters with API mass fraction is difficult to model and has little impact on the predictability of the roller compactor model.

In Section 4.2.1, the tablet press process model and tablet tensile strength material model were calibrated to predict the compressibility and compactability of the formulation as a function of API mass fraction. The compressibility model describes the densification of the formulation mixture as a function of applied pressure (Eq. (3)), but uses a different functional form to the roller compaction process model (Eq. (1)). The calibrated compressibility model was used to generate pressure/porosity profiles for different API mass fractions and these were fitted to a linearised version of Eq. (1) in order to estimate K_T' and $\gamma_{0,T}$ (Eq. (17)):

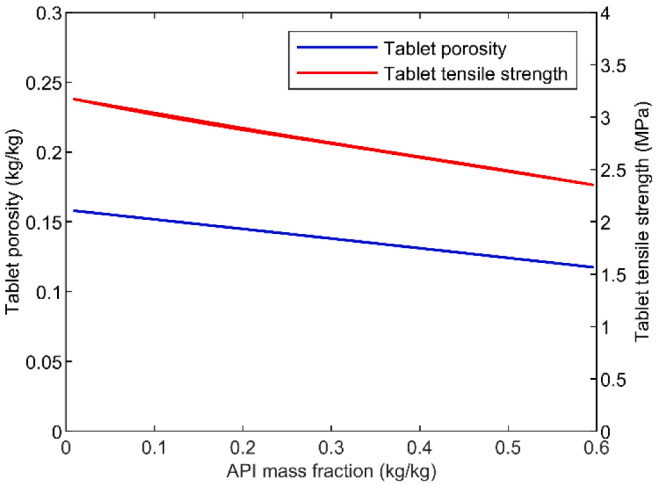

Fig. 4. Tablet porosity and tablet tensile strength as a function of API mass fraction in the RC system at a tablet press compaction pressure of 150 MPa, a roll force per width of roll of 5 kN/cm and a roll gap of 2 mm as predicted by the (Reynolds et al., 2017) model.

Table 5
Model parameters for calibrating the RC model based on 40% w/w blend shear cell (measured at a pre-consolidation stress of 4 kPa).

Parameter	Value
Effective angle of internal friction, δ_E	48.2°
Angle of wall friction, ϕ_W	15.7°

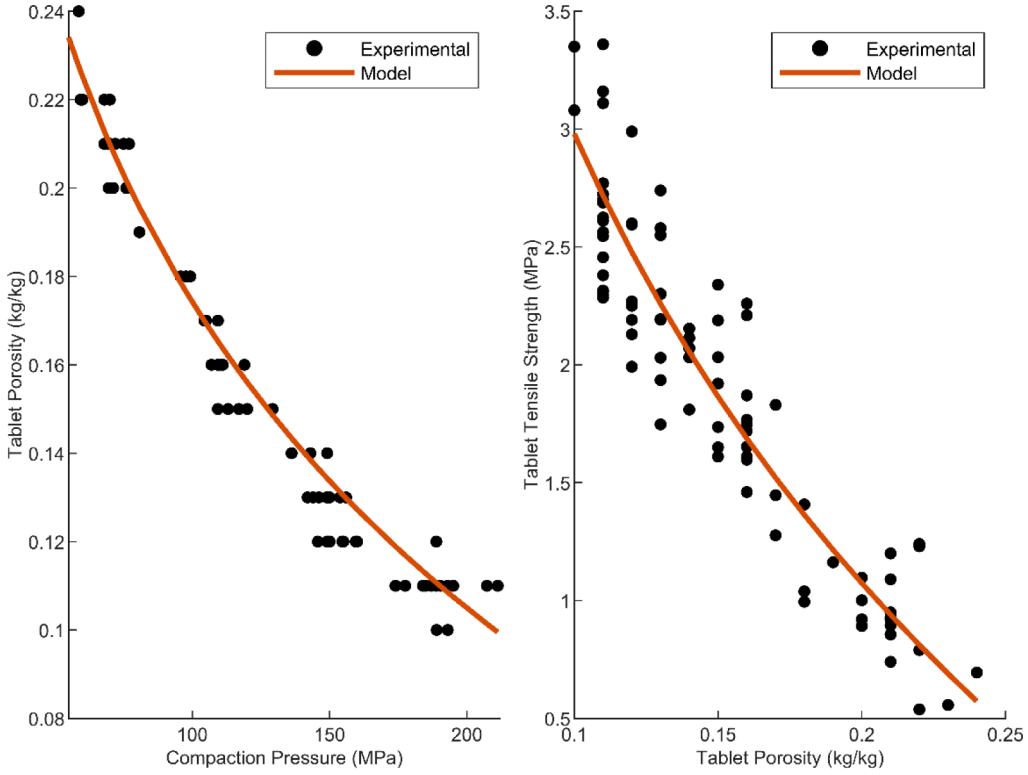

Fig. 3. (a) Compressibility and (b) compactability models comparing experimental 40% w/w API mass fraction compaction data (dots) and the model fitted with the back fitting procedure (line).

$$\ln(1-\epsilon_{tablet}) = \frac{1}{K_T'}\ln(P) + ln(\gamma_{0,T}) \quad (17)$$

This now gives us parameters that could be used in the RC process model. However, due to the partially-confined compression experienced in the roller compactor, the ribbon will exhibit a lower extent of densification for an applied normal pressure compared with a tablet in a confined die. Therefore additional coefficients were included to modify the parameters derived from tablet compression for use in the RC process model (Eq. (2)) as shown in Eqs. (18) and (19):

$$\gamma_0 = c_{\gamma_0}\gamma_{0,T} \quad (18)$$

$$K_{RC} = c_K K_T' \quad (19)$$

A large dataset for roller compacted 40% w/w blends were used to fit the correction factors, with expected values between 0 and 1.

The sum of square errors (SSE) between measured and predicted ribbon porosities was minimized by adjusting the correction factors c_{γ_0} and c_K using a GRG non-linear solver. The predicted maximum pressure at minimum separation (P_{max}) is also a function of the roller compactor model parameters and therefore several iterations were carried out to converge the model parameters. To determine the goodness of the fit of the corrected RC parameters, the experimental vs predicted ribbon porosity graph was produced at 40%w/w API mass fraction in Fig. 5.

The ribbon density model was fitted using all of the available data to yield an RMSE of 9.9% and 3.1% for the uncorrected and corrected relative ribbon density models, respectively. To partly validate and assess the predictability of the model, the dataset was split into a calibration set ($n = 39$) and a validation set ($n = 22$). RMSEC was 3.3% for the corrected relative ribbon density models, with an RMSEP of 2.9%. These metrics demonstrate the reliability of the model and the potential to utilize a smaller dataset for model calibration. The parameters fitted from the full dataset are used for the remainder of this study. It is worth noting that there is significant variability in the experimental data due to variability in ribbon porosity measurements using the Geopyc. The addition of the multiplicative correction factors significantly improves the fit through a reduced RMSE. Values for $\gamma_0$and K_{RC} were fitted for 61 values of API mass fraction between 0.60%w/w. A polynomial relationship existed between γ_0 and K_{RC} and API mass fraction and the coefficients of the polynomial curve were fitted for both parameters to be used for future predictions.

A polynomial equation for γ_0 vs. x_{API} was fitted with an R^2 of 1.0 (Eq. (20))

$$\gamma_0 = 0.105{x_{API}}^2 + 0.172x_{API} + 0.259 \quad (20)$$

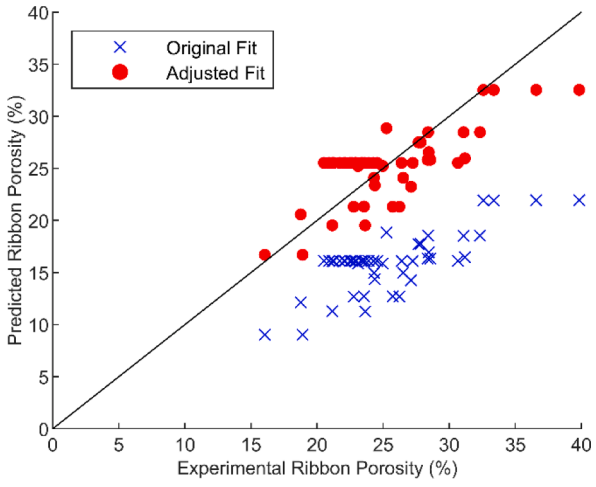

Fig. 5. Parity plot for back fitted roller compactor model comparing the uncorrected and correct models.

A polynomial equation for K_{RC} vs. x_{API} was fitted with an R^2 of 1.0 (equation 20)

$$K_{RC} = 5.549{x_{API}}^2 + 1.937x_{API} + 4.249 \quad (21)$$

5. Results and discussion

5.1. Model system analysis

A calibrated system model was used to predict the impact of different factors on the model responses. All factors were varied in a uniform distribution between the lower and upper limits stated in Table 6. Sobol sampling was used to select factor values for simulations. The bounds of the factors were varied to purposely induce failure in a high number of the responses in order to fully explore the failure modes of the system and determine the edge of failure.

The model system analysis was performed twice for two different sized tablets to determine the impact of tablet size on the dosage and API mass fraction requirements for process selection. The tablet die dimensions used in the tablet press unit operation model were: an 800 mg 9 × 18 mm concave oval tablet, to represent the maximum tablet size that would be reasonable acceptable and a 400 mg 6 × 12 mm concave oval tablet, to explore the impact of a smaller tablet size which may be required for different patient populations.

5.2. System constraints for feasible design space

When exploring the design space for a given system model, each response has defined requirements based on process and product robustness. All responses of the model, blend bulk density and FFC, ribbon and tablet porosity and tensile strength and die fill level, have defined requirements that are based on the MCS (Leane et al., 2015, 2018) and industrial experience.

5.2.1. Tablet and ribbon properties

The tensile strength of the ribbon should be more than 0.8 MPa to ensure sufficient compaction to form a coherent ribbon and ensure adequate mechanical strength to produce granules from milling based on industrial experience. Eq. (8) was used to determine the ribbon tensile strength.

To avoid over-compression and capping of a tablet, the tablet porosity should not exceed the value at which the compaction profile begins to deviate from Eq. (3). For the experimental data used to calibrate the model, over-compression occurs around 0.92 kg/kg solid fraction of 0.08 kg/kg tablet porosity. This is supported by a recommended solid fraction of 0.85± 0.05 kg/kg by Hancock et al. (2003). The tablet porosity limit was therefore set at > 0.08 kg/kg. The tablet tensile strength should be > 1.7 MPa to ensure robust downstream processing of the tablets such as coating, packaging, transport and patient handling (Pitt and Heasley, 2013; Leane et al., 2015).

5.2.2. Bulk material properties

The MCS states that the bulk density of the blend should ideally be > 200 kg m^{-3} for a robust RC manufacturing process (Leane et al., 2015). For direct compression, the risk associated with bulk density is determined by calculating the die fill level in Eq. (5). Based on industrial

Table 6
Factors varied in the system model analysis.

Factor	Units	Bounds
API bulk density	kg m^{-3}	50–600
API FFC	–	1.0–5.0
API mass fraction	kg/kg	0.10–0.60
Tablet compaction pressure	MPa	50–300
Roll force	kN/cm	2.0–10.0
Roll gap	mm	1.0–6.0

experience, a common tablet die has a maximum powder level of 19 mm. Therefore, die fill level < 19 mm was implemented into the design space exploration.

The FFC is a measure of how flowable powder is and therefore an indication of processing risk. For a robust RC process, the blend FFC should be > 4 (Leane et al., 2015; Kalaria et al., 2020) which aligns with the FFC value classification outlined by Schulze (2008). However, previous industrial experience has shown that there is some leniency in the value, depending on equipment configuration, so blend FFC as low as 3 was considered potentially feasible for RC, but with some potential risk.

Flow is more critical for process and product robustness for direct compression compared with roller compaction. The die fill level calculation (Eq. (5)) only considers bulk density as a risk factor in the tablet press. Therefore, any risk associated with flow must be implemented as a constraint on the blend FFC. Whilst the MCS (Leane et al., 2015) and the review of real life applications of the MCS (Leane et al., 2018) have no specific recommendations for blend FFC for direct compression, the internal industrial experience of DC aims for FFC> 5 to reduce any processing risks.

5.3. Design space visualization and quantification

Model system analyses was performed with the number of simulated batches varied between 500 and 7000. The simulated batches were then grouped into 10% w/w API mass fraction intervals and the probabilities of a simulated batch meeting each constraint and all of the response constraints was calculated for each API mass fraction interval. This was repeated for different numbers of simulated batches within a given system analysis. It was found that the probabilities converged as the number of simulated batches increased above 6000.

The results of the system analyses were used to produce process classification maps based on flowability, bulk density and die fill level requirements. The results were also used to generate a design space map for identifying the robust operating space for the roller compaction manufacturing process. To visualize the constraints outlined in Table 7, the regime maps were colored based on whether simulated batches met a specified set of responses.

5.3.1. Process classification maps

Process classification maps (Figs. 6, 7) can be used to determine the feasibility of different OSD manufacturing processes based on API material properties and dosage requirements, enabling decisions to be made around the most suitable drug product process route. The process classification maps were developed using sub-sets of the system analysis outputs.

Figs. 6 and 7 are plots of the impact of API FFC, API bulk density and API mass fraction on the risk of tablet manufacturing via roller compaction and direct compression. For some powders it might be reasonable to expect a correlation between API bulk density and API FFC, but not correlation was found in the dataset and therefore these properties were varied independently. The quantitative visualizations produced here are specific to the formulation used to calibrate the model, however the qualitative trends are expected to be more generally applicable. The process classification maps consider DC, RC and other manufacturing technologies, which correspond with class I, class II and class III and IV combined respectively in the MCS (Leane et al., 2015).

Table 7
Responses specified as outputs of the system model analysis and their corresponding constraints.

Responses	Units	Required Range	Source
Ribbon tensile strength	kg m^{-3}	> 0.8	Industrial experience
Tablet porosity	kg/kg	> 0.08	Experimental observation of over-compression
Tablet tensile strength	MPa	> 1.7	MCS (Leane et al., 2015, 2018)
Blend bulk density	kg m^{-3}	RC: > 200	MCS (Leane et al., 2015, 2018)
Blend FFC	–	DC: > 5 RC: > 4 RC with potential risk: >3	Schulze (2008) and industrial experience
Die fill level	mm	<19	Industrial experience

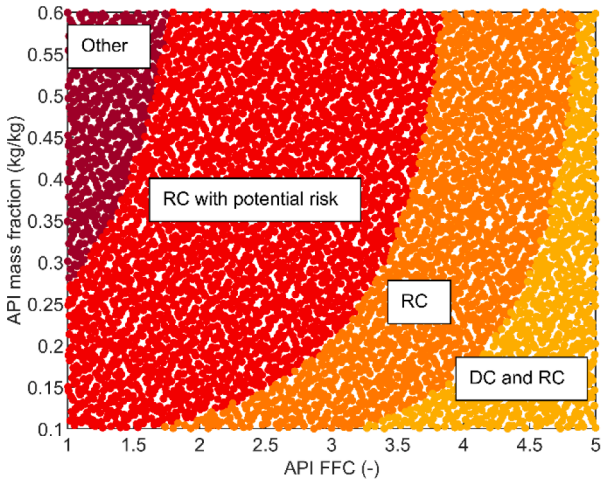

Fig. 6. Process classification map showing the regions of API FFC (measured at a pre-consolidation stress of 4 kPa) and API mass fraction (kg/kg) required for DC and RC processing based on blend FFC requirements.

The FFC process classification map in Fig. 6 was constructed using the API FFC and API mass fraction factors with blend FFC as the only response. The map is colored by the response requirements (Table 7). The bulk density process classification map (Fig. 7) was constructed using the API bulk density, API mass fraction and dosage factors and the blend bulk density and die fill level responses. The map is colored to indicate a favorable region for both direct compression and roller compaction, defined by the die fill level requirements (Table 7). The regions favorable to only RC and other manufacturing technologies regions are defined by the blend bulk density constraint (Table 7).

Process classification maps can be used to guide development of drug product. The following discussion provides some examples of the design questions asked during product development and how the process classification maps can be used to support these development decisions.

Which processing route is the most robust given the API material properties and dosage requirements?: Fig. 6 can be utilized to assess the flowability risk and Fig. 7 can be utilized to assess the bulk density risk associated with a new API for a given manufacturing method and therefore identify the most suitable drug product processing route based on dosage requirements. For a fixed dosage and API bulk density, Fig. 7 can be used to assess which API mass fraction is required for the formulation for a given tablet size and whether direct compression, roller compaction or an alternative manufacturing route is the most suitable. At low API properties and high API mass fraction, the unfavorable bulk properties dominate the blend bulk properties and therefore more complex process routes with less sensitivity to physical properties are more favorable as the appropriate manufacturing route.

How does drug loading and tablet size impact the robustness of the manufacturing process?: API mass fraction and tablet size are two factors that influence the feasibility of different manufacturing routes which can be altered during formulation development. Therefore, Fig. 6 can be used to assess which API mass fraction is required to facilitate direct compression. An API with an FFC of 4 is likely to have sufficient flow properties to perform robustly during roller compaction for this formulation, whereas a API mass fraction of less than 20% w/w would be required to ensure a robust DC process with respect to flow into the tablet die. Fig. 6 builds upon the process flow maps produced by Leane

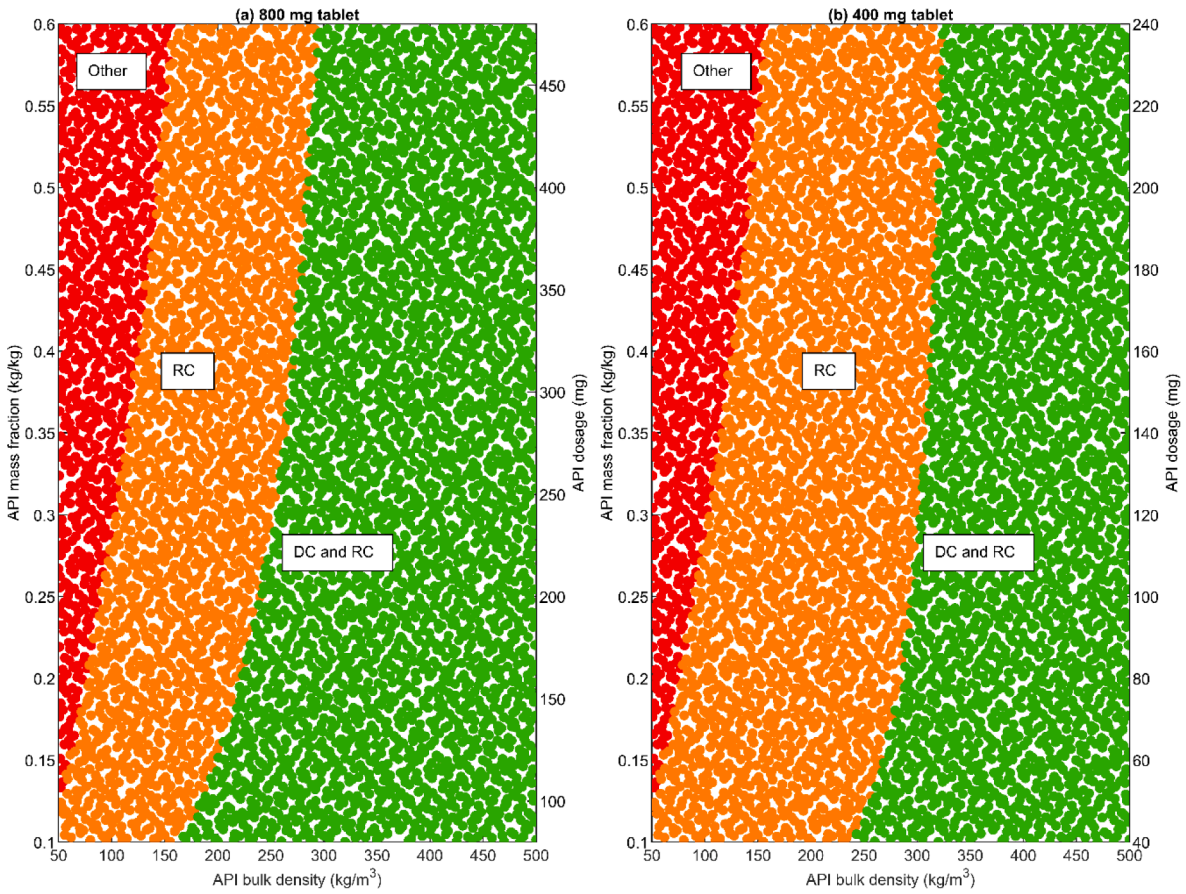

Fig. 7. Process classification map showing the regions of API bulk density and API mass fraction (% w/w) required for DC and RC processing based on blend bulk density and die fill level for a (a) 800 mg oval tablet and a (b) 400 mg oval tablet.

et al. (2018) where the different processing routes used by AstraZeneca drug products as a function of API FFC and API mass fraction were plotted. Fig. 6 shows the same trends as the work by Leane et al. (2018) and provides a more comprehensive understanding of the design space produced without extensive experimental work.

Tablet size and number of tablets form part of patient centric pharmaceutical drug product design when trying to improve medication adherence (Menditto and Orlando, 2020) and should be considered when making process and formulation design decisions. Here, we took an 800 mg oval tablet as the maximum size suitable for a general patient population. Certain patient populations, however, may have requirements for limits on tablet size and process classification maps can be used to evaluate the impact of smaller tablet requirements on feasibility of manufacturing routes. During early clinical studies, a range of doses is required to determine the optimal therapeutic window for a given API. Process classification maps can also be used to assess whether a given manufacturing route is feasible for given API properties and the range of doses required to support these studies. To achieve the same dosage in a single smaller tablet size, a higher API mass fraction is required. Therefore, a smaller feasible design space for DC is available for the 400 mg tablet compared to the 800 mg tablet (Fig. 7). However, the maximum dosage that can be achieved is lower for a 400 mg tablet (240 mg at 60% w/w API mass fraction) compared with a 800 mg tablet (300 mg at a 60% w/w API mass fraction), so a compromise must be made on tablet size, number of tablets and the desired manufacturing route.

Process classification maps enable patient-centric formulation and manufacturing design through the visualization of the API mass fraction and tablet size requirements to achieve a target dosage. To achieve a selected manufacturing pathway, process classification maps can be used to holistically identify where process development should be focussed: appropriate particle engineering to improve API physical properties (Mirza et al., 2009; Perumalla and Sun, 2014; Wilson et al., 2018) or adjustments to the formulation and tablet size to de-risk the manufacturing route. For example, target criteria for API physical properties can be identified if a specific API mass fraction and manufacturing process are desired. Additionally, process classification maps provide a simple methodology for determining the risk associated with a manufacturing process for given API properties and fixed formulation.

5.3.2. *Roller compaction design space map*

The model system analysis outputs were used to generate a design space map for identifying a robust operating space for the RC manufacturing process as a function of API FFC and API mass fraction. Understanding the impact of both material properties and process parameters on the critical quality attributes of the process can be used to make decisions about the appropriate range of process parameters required to achieve a robust process design space.

The design space map (Fig. 8) can be used to assess the API properties, formulation and process parameter requirements required to achieve a robust roller compaction process. It was constructed using the API FFC, API mass fraction, roll force, roll gap and compaction pressure factors. Blend FFC, ribbon tensile strength, tablet porosity and tablet tensile strength responses and their corresponding constraints were used to define the robust operating region for an RC process. While API bulk density, as a function of API mass fraction, impacted the blend bulk density, it was excluded from Fig. 8 for simplicity to focus on the most practically important factors and responses.

Fig. 8 is a plot of all 6000 simulated batches from the model system

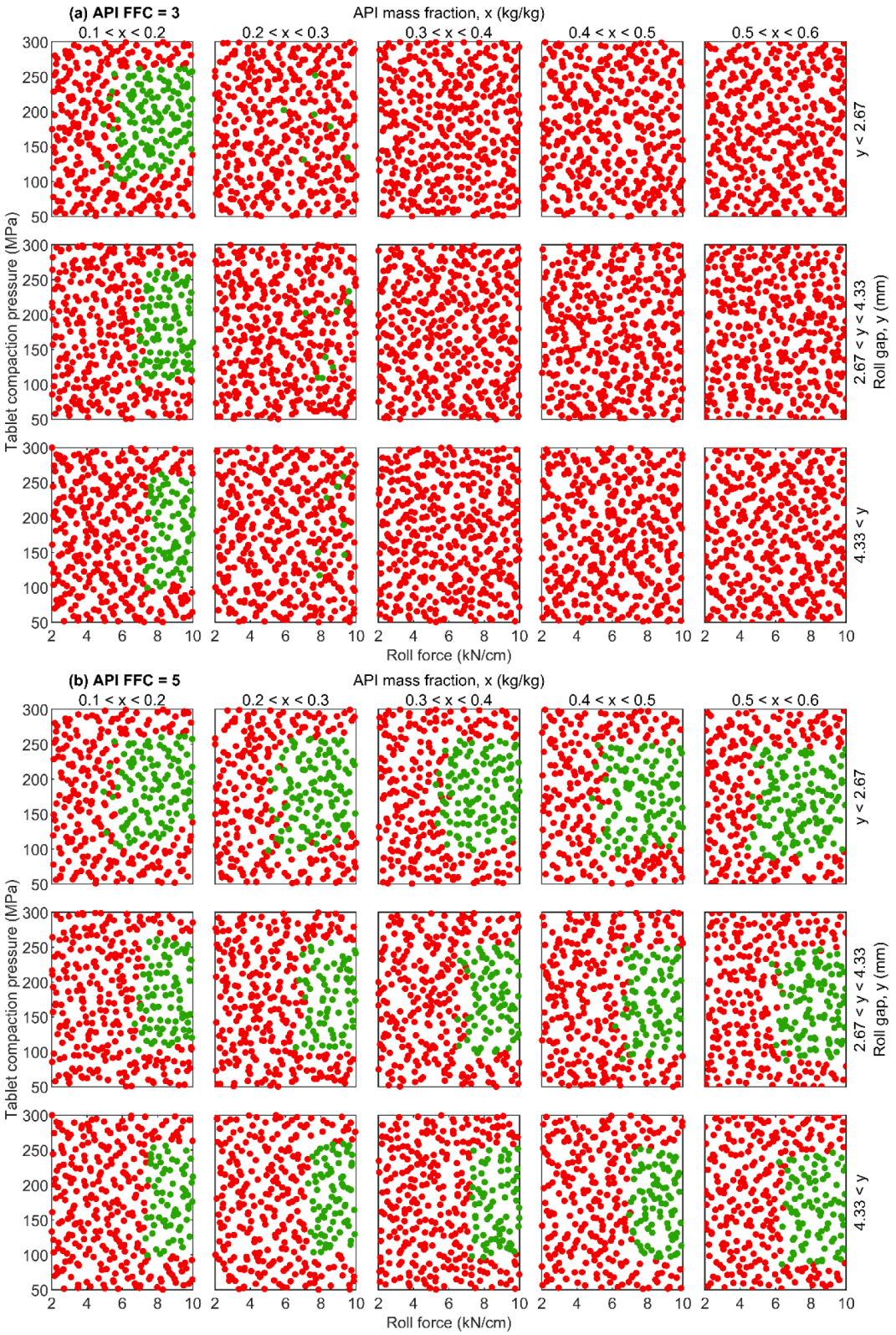

Fig. 8. Design space maps for the RC process as a function of roll force (kN/cm), roll gap (mm), tablet press compaction pressure (MPa), API mass fraction (kg/kg) and API FFC. API FFC factor range is constrained to 2 discrete values: (a) 3 and (b) 5. All 6000 simulated batches from the model system analysis are shown on the plot, where green indicates that the simulated batch meet all of the specified material and product constraints, and red indicates that at least one constraint was violated.

analysis, where green indicates that the simulated batch meets all of the specified material and product constraints, and red indicates that at least one constraint was violated. At the boundary of the feasible reason, there is a 50% chance of a given simulated batch meeting all of the criteria and caution should be taken operating at the edge of this boundary due to this uncertainty.

Design space maps can be used to guide development of drug product manufacturing process. The following discussion provides some examples of the design questions asked during the development of the roller compaction process and how the design space maps can be used to support these development decisions.

What process settings are required for a robust manufacturing route for the API material properties and drug loading requirements?: For a given set of API flowability and API mass fraction requirements, Fig. 8 can be used to evaluate the operating space for the RC process, where the green region indicates the range of roll force, roll gap and tablet compaction pressure values which produce ribbons and tablets within specification (Table 7). The design space map can be utilized to identify an appropriate set point for the RC and tablet press to ensure a robust process without extensive experimentation.

How does drug loading impact the robust manufacturing route operating space?: API mass fraction is an important factor during process selection (Figs. 6, 7), dosage regime design (Fig. 7) and process robustness (Fig. 8). When changes to API mass fraction need to be made to facilitate a robust manufacturing process or specific dosage requirements, the impact on the operating space of the manufacturing process needs to be evaluated to present the critical product attributes falling out of specification. For the system model, the probability of a simulated batch meeting 1 or all of the blend FFC, ribbon tensile strength, tablet porosity and tablet tensile strength criteria in Table 7 as a function of API mass fraction was determined. The number simulated batches in a given API mass fraction interval which met each or all of the criteria over the total number of points in the API mass fraction interval was calculated, and is presented in Fig. 9.

If 6000 simulated batches are generated across the respective full ranges of the factors stated above, the probability of meeting all the criteria is highest (16%) when API mass fraction is restricted to 10–20% w/w (Fig. 9). Low API mass fraction reduces the impact of poor API properties on the blend properties, therefore increases process robustness and maximizes the feasible operating space. Primarily, this is dominated by the blend FFC constraint, which is only dependent on API FFC and API mass fraction as demonstrated by a significantly larger region of feasible RC manufacturing at 10–20%w/w API mass fraction in Fig. 6. A large difference is seen in the number of simulated batches which meet all of the criteria between API FFC values of 3 and 5. For a robust roller compaction process, the blend FFC should be greater than 4 (Table 7). For an API FFC of 5, all simulated batches meet the blend FFC criteria. For an API FFC of 3, only the API mass fraction range of 10–20% w/w has simulated batches which meet the blend FFC criteria, with a very small number of simulated batches with API mass fraction 20–30% w/w. Therefore, if the flowability of the API is poor (i.e. less than 4) then there is risk to the process robustness unless a API mass fraction $< 0.2\%$ w/w is used.

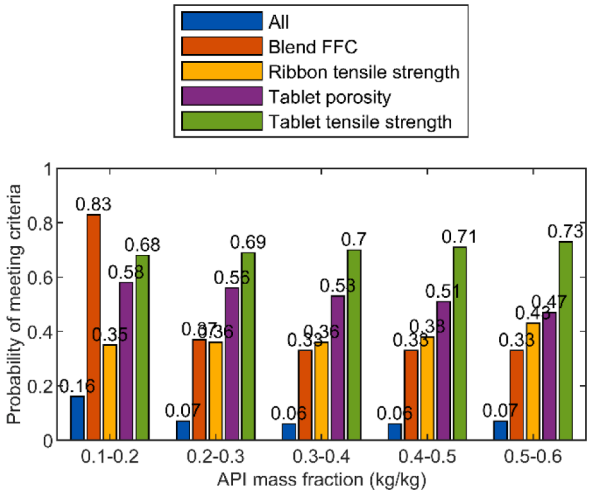

Fig. 9. Probability of meeting each criteria in the roller compactor system as a function of API mass fraction. API mass fraction is constraints to 10% w/w intervals. API bulk density is excluded and API FFC is constrained to two discrete values: 3 and 5. All factors except API mass fraction are averaged across their full range.

Fig. 9 quantifies the probability of a simulated batch meeting all of the criteria and a breakdown of the probability of meeting each criteria within a API mass fraction interval. During the calibration of the tablet porosity and tablet tensile strength models, API mass fraction had limited impact on the tablet porosity and tablet tensile strength (Fig. 4). Therefore, the probability of meeting the tablet tensile strength criteria shows weak positive correlation with API mass fraction and the probability of meeting the tablet porosity criteria shows weak negative correlation with API mass fraction (Figs. 8, 9). If 6000 samples are taken across the respective full ranges of all factors stated above, the probability of meeting the tablet porosity criteria decreases from 58% when API mass fraction is restricted to 10–20%w/w to 47% when API mass fraction is restricted to 50–60%w/w due to a shift in the design space (Fig. 9). At a higher API mass fraction, a lower compaction pressure is required to achieve the same tablet porosity compared to a lower API mass fraction as the API is more compressible than the excipients.

The probability of meeting the ribbon tensile strength criteria shows a weak correlation with API mass fraction, as expected due to the fitting of the RC model Fig. 9. At a lower API mass fraction, there is a larger range of RC process settings that can be utilized to achieve an in specification ribbon. However, the design space map should not necessarily be used to optimize for the larger feasible area but to indicate where in the design space it is safe to operate and determine how that may change with API mass fraction without further experimental work.

5.4. Model limitations and next steps

The data used to construct the model was based on historical archives of industrial process development data. The data was not specifically generated to calibrate a model but to answer specific material and process questions during development. Although large quantities of data were available due to the processability issues with this particular drug product, it would not be necessary to generate such a large dataset in order to construct a system model for a new API. Any experimental work to calibrate a similar model should focus on a small number of experiments across the breadth of the design. As demonstrated in Section 4.2, the models can be calibrated using a smaller subset of the data utilized in this work, with any additional data used for validation and/or improving fidelity. Table 8 outlines the minimum data requirements for each stage of the manufacturing process required to calibrate the model. The minimum data requirements under the ‘must’ column indicate the minimum data based on having a sufficient degrees of freedom to calibrate the model. The ‘could’ column indicates data which would be required to expand the model further to provide a deeper understanding of the system or further data points which would provide a more accurate calibration on the model.

The tablet manufacturing system model developed here poses some limitations due to the dataset available. It is acknowledged that while API mass fraction was an important factor in the process classification and design space exploration, the model had not been validated outside a singular API mass fraction formulation. Additional validation data and sub-models which describe other phenomena in the system could be added to the framework presented here to expand the scope of the system model and improve confidence in the final process selection and

Table 8
Minimum data requirements to calibrate the individual models of the system model.

	Must	Could
Material characterization	Component (API and excipients): Mass fraction, particle density, bulk density, FFC, compressibility, compactability, effective angle of internal friction, wall friction angle	Blend (at different API mass fractions and/or placebo) Composition, particle density, bulk density, FFC, compressibility, compactability, effective angle of internal friction, wall friction angle
Roller compactor	3 different ribbon porosities from different roll force and roll gap settings 2 different API mass fractions and/or placebo	Additional ribbon porosities and blend formulations
Tablet press	For each ribbon porosity, tablet compaction profiles with tablet porosity and table tensile strength	

design space exploration results.

The focus of the system model explored in this study was on the impact of bulk density, flowability and compaction properties on manufacturability. Within the framework of the work presented, additional models can be incorporated to predict other intermediate and product attributes. For example, the system model could be extended to include the milling unit operation and dissolution performance if required as part of the process evaluation, as demonstrated by Gavi and Reynolds (2014) and Park et al. (2018). The additional process parameters and product quality attributes from milling and dissolution could be added to extend the design space exploration visualization and quantification to more factors and responses.

For simplicity and clarity the simplest manufacturing process presented in the system model was direct compression due to the focus on blend bulk density, flowability and compaction properties. In reality, continuous direct compression is becoming increasingly important as a processing route and this system model can also be used to enable selection of this continuous process. Additional models could be incorporated into the system model framework to explore additional specific criteria for CDC, for example by considering feeder performance, such as models presented by Bostijn et al. (2019), Tahir et al. (2020).

While some of the presented models could be improved and could not be fully validated for API mass fractions other than 40% w/w and a single point at 0% w/w, this proof of concept can be used to establish a framework for exploring the manufacturability design space with a system model. Incorporating improved models would extend the predictability and utility of this approach for process selection and formulation design.

6. Conclusions

A computational framework was developed to generate process classification and design space maps to aid robust pharmaceutical formulation and process decision making. Specifically, a system model was developed to simulate the tablet manufacturing process by both roller compaction and direct compression. 6000 simulations were performed over a range of operating conditions and API material properties. Process classification maps were produced to assess the feasibility of RC and DC for different material properties and formulations. Additionally, constraints on the quality attributes of the intermediate and final products were defined using the Manufacturing Classification System and design space maps were produced to determine the impact of API mass fraction and material properties on the size and shape of the RC robust design space.

Process classification maps have been constructed using a model systems analysis approach. This showed that for direct compression to be feasible, the FFC of the API needs to be relatively high, otherwise granulation processes may be more suitable. Reducing the API mass fraction can help improve the feasibility of direct compression, however in this case study, the API flow properties dominate even when the API component is around 10% w/w. In the case study presented, the API bulk density is the main factor over the selection of manufacturing route, however the dose requirement and flow properties also play a role.

Following on from the process selection, the design space maps presented here demonstrate how system models can be used to support formulation and process design. The design space maps illustrate how the process operating space can be increased or decreased as the API mass fraction is varied.

The process design and selection system model demonstrate how an understanding of the API physical properties can be used to model the impact of formulation and process design. Furthermore, these models can be instrumental in the dialogue with colleagues developing the API in order to set the requirements of the API physical properties to ensure successful and robust formulation and process designs Eqs. (9), ((10), (13), (15), (17)–(21), and (4)).

Declaration of Competing Interest

The authors declare no conflicts of interest.

Acknowledgments

We gratefully acknowledge the support of Innovate UK through the funding of the “Digital Design Accelerator Platform to Connect Active Material Design to Product Performance” (Grant No. 105811) within which the work reported was conducted as part of the AstraZeneca case study for the Innovate UK funded Digital Design Accelerator Platform Project.

Supplementary materials

Supplementary material associated with this article can be found, in the online version, at doi:10.1016/j.ejps.2022.106140.

References

Bostijn, N., Dhondt, J., Ryckaert, A., Szab, 2019. A multivariate approach to predict the volumetric and gravimetric feeding behavior of a low feed rate feeder based on raw material properties. Int. J. Pharm. 557 (December 2018), 342–353.
Chattoraj, S., Sun, C.C., 2018. Crystal and particle engineering strategies for improving powder compression and flow properties to enable continuous tablet manufacturing by direct compression. J. Pharm. Sci. 107 (4), 968–974.
Duckworth, W., 1953. Discussion of ryshkewitch paper by Winston Duckworth. J. Am. Ceram. Soc. 36, 68.
Farber, L., Hapgood, K.P., Michaels, J.N., Fu, X.Y., Meyer, R., Johnson, M.A., Li, F., 2008. Unified compaction curve model for tensile strength of tablets made by roller compaction and direct compression. Int. J. Pharm. 346 (1–2), 17–24.
Gavi, E., Reynolds, G.K., 2014. System model of a tablet manufacturing process. Comput. Chem. Eng. 71, 130–140.
Hancock, B.C., Colvin, J., Mullarney, M.P., Zinchuk, A., 2003. The relative densities of pharmaceutical powders, blends, dry granulations, and immediate-release tablets. Pharm. Technol. 27, 64–80.
Iacocca, R.G., Burcham, C.L., Hilden, L.R., 2010. Particle engineering: a strategy for establishing drug substance physical property specifications during small molecule development. J. Pharm. Sci. 99 (1), 51–75.
Johanson, J.R., 1965. A rolling theory for granular solids. J. Appl. Mech. 32 (4), 842–848.
Kalaria, D.R., Parker, K., Reynolds, G.K., Laru, J., 2020. An industrial approach towards solid dosage development for first-in-human studies: application of predictive science and lean principles. Drug Discov. Today 25 (3), 505–518.
Kushner, J.T., Moore, F., 2010. Scale-up model describing the impact of lubrication on tablet tensile strength. Int. J. Pharm. 399 (1–2), 19–30.
Leane, M., Pitt, K., Reynolds, G., Anwar, J., Charlton, S., Crean, A., Creekmore, R., Davies, C., DeBeer, T., De-Matas, M., Djemai, A., Douroumis, D., Gaisford, S., Gamble, J., Stone, E.H., Kavanagh, A., Khimyak, Y., Kleinebudde, P., Moreton, C., Paudel, A., Storey, R., Toschkoff, G., Vyas, K., 2015. A proposal for a drug product

manufacturing classification system (MCS) for oral solid dosage forms. Pharm. Dev. Technol. 20 (1), 12–21.
Leane, M., Pitt, K., Reynolds, G.K., Dawson, N., Ziegler, I., Szepes, A., Crean, A.M., 2018. Manufacturing classification system in the real world: factors influencing manufacturing process choices for filed commercial oral solid dosage formulations, case studies from industry and considerations for continuous processing. Pharm. Dev. Technol. 23 (10), 964–977.
Lee, B.K., Yun, Y., Park, K., 2016. PLA micro- and nano-particles. Adv. Drug Deliv. Rev. 107, 176–191.
Lee, B.W., Peterson, J.J., Yin, K., Stockdale, G.S., Liu, Y.C., O-Brien, A., 2020. System model development and computer experiments for continuous API manufacturing. Chem. Eng. Res. Des. 156, 495–506.
Lee, S.L., O'Connor, T.F., Yang, X., Cruz, C.N., Chatterjee, S., Madurawe, R.D., Moore, C. M.V., Yu, L.X., Woodcock, J., 2015. Modernizing pharmaceutical manufacturing: from batch to continuous production. J. Pharm. Innov. 10 (3), 191–199.
Mascia, S., Heider, P.L., Zhang, H., Lakerveld, R., Benyahia, B., Barton, P.I., Braatz, R.D., Cooney, C.L., Evans, J.M.B., Jamison, T.F., Jensen, K.F., Myerson, A.S., Trout, B.L., 2013. End-to-end continuous manufacturing of pharmaceuticals: integrated synthesis, purification, and final dosage formation. Angew. Chem. Int. Ed. 52 (47), 12359–12363.
Menditto, E., Orlando, V., 2020. Patient centric pharmaceutical drug product design-the impact on medication adherence. Pharmaceutics 12 (1), 1–23.
Mirza, S., Miroshnyk, I., Heinmki, J., Antikainen, O., Rantanen, J., Vuorela, P., Vuorela, H., Yliruusi, J., 2009. Crystal morphology engineering of pharmaceutical solids: tabletting performance enhancement. AAPS PharmSciTech 10 (1), 113–119.
Palmer, J., Reynolds, G.K., Tahir, F., Yadav, I.K., Meehan, E., Holman, J., Bajwa, G., 2020. Mapping key process parameters to the performance of a continuous dry powder blender in a continuous direct compression system. Powder Technol. 362 (December), 659–670.
Park, S.Y., Galbraith, S.C., Liu, H., Lee, H.W., Cha, B., Huang, Z., O'Connor, T., Lee, S., Yoon, S., 2018. Prediction of critical quality attributes and optimization of continuous dry granulation process via flowsheet modeling and experimental validation. Powder Technol. 330, 461–470.
Perez-Gandarillas, L., Perez-Gago, A., Mazor, A., Kleinebudde, P., Lecoq, O., Michrafy, A., 2016. Effect of roll-compaction and milling conditions on granules and tablet properties. Eur. J. Pharm. Biopharm. 106, 38–49.
Perumalla, S.R., Sun, C.C., 2014. Enabling tablet product development of 5-fluorocytosine through integrated crystal and particle engineering. J. Pharm. Sci. 103 (4), 1126–1132.
Pishnamazi, M., Casilagan, S., Clancy, C., Shirazian, S., Iqbal, J., Egan, D., Edlin, C., Croker, D.M., Walker, G.M., Collins, M.N., 2019. Microcrystalline cellulose, lactose and lignin blends: process mapping of dry granulation via roll compaction. Powder Technol. 341, 38–50.
Pitt, K.G., Heasley, M.G., 2013. Determination of the tensile strength of elongated tablets. Powder Technol. 238, 169–175.
Pitt, K.G., Newton, J.M., Stanley, P., 1989. Stress distributions in doubly convex cylindrical discs under diametral loading. J. Phys. D Appl. Phys. 22 (8), 1114–1127.
Pohl, S., Kleinebudde, P., 2020. A review of regime maps for granulation. Int. J. Pharm. 587 (July), 119660.
Reynolds, G., Ingale, R., Roberts, R., Kothari, S., Gururajan, B., 2010. Practical application of roller compaction process modeling. Comput. Chem. Eng. 34 (7), 1049–1057.
Reynolds, G.K., Campbell, J.I., Roberts, R.J., 2017. A compressibility based model for predicting the tensile strength of directly compressed pharmaceutical powder mixtures. Int. J. Pharm. 531 (1), 215–224.
Schulze, D., 2008. Powders and Bulk Solids. Springer.
Souihi, N., Josefson, M., Tajarobi, P., Gururajan, B., Trygg, J., 2013. Design space estimation of the roller compaction process. Ind. Eng. Chem. Res. 52 (35), 12408–12419.
Sun, C.C., Kleinebudde, P., 2016. Mini review: mechanisms to the loss of tabletability by dry granulation. Eur. J. Pharm. Biopharm. 106, 9–14.
Tahir, F., Palmer, J., Khoo, J., Holman, J., Yadav, I.K., Reynolds, G., Meehan, E., Mitchell, A., Bajwa, G., 2020. Development of feed factor prediction models for loss-in-weight powder feeders. Powder Technol. 364, 1025–1038.
Vercruysse, J., Delaet, U., 2013. Stability and repeatability of a continuous twin screw granulation and drying system. Eur. J. Pharm. Biopharm. 85 (3 PART B), 1031–1038.
Wilson, D., Bunker, M., Milne, D., Jawor-Baczynska, A., Powell, A., Blyth, J., Streather, D., 2018. Particle engineering of needle shaped crystals by wet milling and temperature cycling: optimisation for roller compaction. Powder Technol. 339, 641–650.
Yu, J., Xu, B., Zhang, K., Shi, C., Zhang, Z., Fu, J., Qiao, Y., 2019. Using a material library to understand the impacts of raw material properties on ribbon quality in roll compaction. Pharmaceutics 11 (12), 662–687.